Structural elucidation of Bisphenol E and S photoinduced by-products by high-resolution electrospray ionisation-mass spectrometry and tandem mass spectrometry

Structural elucidation of Bisphenol E and S photoinduced by-products by high-resolution electrospray ionisation-mass spectrometry and tandem mass spectrometry

M. Coha[1], F. Dal Bello[2], D. Fabbri[1], P. Calza[1*], C. Medana[2]

[1] Chemistry Dept., Università degli Studi di Torino, Via Pietro Giuria 5, 10125 Turin, Italy.

[2] Molecular Biotechnology and Health Sciences Dept., Università degli Studi di Torino, Via Pietro Giuria 5, 10125 Turin, Italy.

Corresponding author: paola.calza@unito.it

ABSTRACT

Rationale: Bisphenol E (BPE) and bisphenol S (BPS) have recently replaced bisphenol A as monomers for producing polycarbonates. However, BPE and BPS can pose hazards as they are known to be endocrine disruptors. Despite the huge increase in their use, there is a lack of data regarding the toxicity and effects of BPE and BPS.

Methods: We investigated the photoinduced transformation of bisphenol E (BPE) and bisphenol S (BPS) when subjected to sun-simulated radiation and using TiO_2 as a photocatalyst. Analyses of BPE, BPS and their by-products were performed by HPLC-HRMS equipped with an orbitrap analyzer in ESI negative mode. The chromatographic separations were achieved by employing a C18 reverse phase column, and the transformation products (TPs) were elucidated structurally using high resolution MS and multistage MS experiments performed in CID mode.

Results: The transformation of bisphenol S involved the formation of twelve by-products, while ten TPs were detected following BPE degradation. For bisphenol S, the cleavage of the molecule is a very important transformation route, together with the hydroxylation of the substrate to provide mono- and poly-hydroxylated TPs. For bisphenol E, the two main routes were hydroxylation and the ring opening. Acute toxicity for BPS, BPE and their transformation products was assessed using *Vibrio fischeri* assay, highlighting that their initial transformation involved the formation of TPs that were more toxic than the parent compound.

Conclusions: The HPLC/HRMS method developed was useful for characterising and identifying newly-formed TPs from bisphenol E and bisphenol S. This study aimed to examine the structure of twenty by-products identified during TiO_2 mediated photolysis and to evaluate acute toxicity over time.

Keywords: bisphenol E, bisphenol S, HPLC/HRMS, transformation products

1. INTRODUCTION

Bisphenols are among the most frequently used monomers for the preparation of polycarbonates (PCs) which, thanks to their excellent properties, are used in a broad spectrum of applications[1].

Traditionally, the most frequently used monomer was bisphenol A (BPA), the demand for which increased over time and reached an estimated global consumption volume of 7.7 million metric tonnes by 2015[2]. The increased production of BPA led to its presence in a large number of environmental matrices, such as sediments and surface and groundwater[3,4], thus becoming one of the five most frequently detected organic substances in groundwater[2,5]. BPA has recently been associated with several diseases, such as obesity, diabetes and breast cancer, and it acts as an endocrine disruptor, provoking reproductive disorders in both sexes[6–8]. These side effects have led to the gradual replacement of this monomer in production lines: for instance, in the last decade, the use of BPA for manufacturing children's products was banned in several countries[9,10].

The use of BPA has been replaced by other bisphenols having similar features, namely bisphenol E (BPE) and bisphenol S (BPS)[11]. BPS is quite soluble in water (1774 mg/L) and has an octanol-water partition coefficient (log K_{ow}) of 1.65-2.14[12], whereas BPE has a log K_{ow} =3.19 [11] and low solubility in water (99 mg/L)[13]. Recently, BPS has been found in the river waters of some Asian countries at concentrations ranging from 8.7 ng/L in India up to 41 ng/L in Korea's Han river[14]. Even through its concentration level is lower than BPA, it still poses concerns. Moreover, its average concentration at the inlet of wastewater treatment plants reaches 55.7 ng/L in China and 14.7 ng/L in India while, after treatment, this is reduced to 3.02 ng/L and 2.4 ng/L, with process efficiencies up to 95% and 84%, respectively[14,15].

For BPE, the concentrations detected at the inlet and outlet of wastewater treatment plants are significantly lower than those of BPA and BPS. Data available for the Xiamen City plant in China reveal an average inlet concentration of 4.51 ng/L. However, despite the high abatement efficiency noted for BPS, in the case of BPE the concentration at the outlet is 4.07 ng/L, thus implying efficiency of about 10%. In some samples, an outgoing concentration higher than at the inlet was observed. This may be caused by fluctuations in the concentration of BPE due to the time taken for complete recirculation of the fluids inside the reactor or the release of analyte previously adsorbed by the walls of the container in which the abatement process is carried out during degradation[16].

BPS and BPE were also found to be endocrine disruptors, with effects generally similar to those displayed by BPA[17,18], thus suggesting that their alternative use could pose risks. Despite the vast amount of literature available for BPA environmental transformation, to the best of our knowledge, no data are available on the effects of BPS and BPE. Therefore, we aim to investigate the nature of photoinduced transformation products (TPs) to assess the abiotic environmental transformations that may occur after their discharge into environmental waters. With this is mind, we used HPLC-HRMS which allowed us to characterise the by-products formed during the irradiation process. To facilitate the structural characterisation, we worked at a higher concentration level (ppm) and we used a photocatalyst to simulate indirect phototransformations of the two molecules, this being a useful and effective approach already used in previous works[19].

2. EXPERIMENTAL SECTION

2.1. MATERIALS

Bisphenol S (CAS 80-09-1, purity ≥ 98%), bisphenol E (CAS 2081-08-5, purity ≥ 98%), acetonitrile and ammonium acetate were all purchased by Sigma Aldrich (Milan, Italy). Experiments were carried out using TiO_2 Evonik P25 (Frankfurt, Germany) as photocatalyst. HPLC-grade water was from MilliQ System Academic (Millipore, Milan, Italy). Acetonitrile was filtered through a 0.45 µm filter before use.

2.2. Irradiation processes

Bisphenol E and S photocatalytic degradation in water was carried out in Pyrex glass cells (2.3 cm × 4.0 cm), filled with 5 mL of analyte (20 mg L^{-1}) and TiO_2 (400 mg L^{-1}) suspension kept under magnetic stirring. The samples were irradiated for different periods using a sun simulator (Solarbox, CO.FO.ME.GRA., Milan, Italy) equipped with a cut-off filter at 340 nm[20]. After irradiation, the samples were filtered through a 0.45 µm filter (Merck Millipore, Milan, Italy) and analysed with a suitable analytical technique.

2.3. Analytical procedures

The degradation of bisphenol E and S and the identification of their TPs in ultrapure water were performed using an Ultimate 3000 High Performance Liquid Chromatography (Thermo Scientific, Milan, Italy) coupled through an ESI source to a LTQ-orbitrap mass spectrometer (Thermo Scientific, Bremen, Germany). Chromatographic separation was achieved with a reverse phase C18 column (Gemini NX C18, 150 × 2 mm, 3 µm, 110 Å; Phenomenex, Castel Maggiore, Bologna, Italy) using 5 mM aqueous ammonium acetate (eluent A) and acetonitrile (eluent B). Gradient separation ramp started with 5% B, increased up to 40% B in 18 minutes and up to 100% in 5 minutes; the column then returned to its initial condition.

The LC effluent was delivered to the ESI ion source using nitrogen both as sheath and as auxiliary gas. The source parameters were set as followed: sheath gas 30 arbitrary unit (arb), auxiliary gas 25 arb, capillary voltage 4.0 kV and capillary temperature 275°C. Full mass spectra were acquired in negative ion mode in the *m/z* range between 50 and 500, with a resolution of 30k. MS^n spectra were acquired in the range between ion trap cut-off and precursor ion *m/z* values. Mass accuracy of recorded ions (versus calculated) was ±0.001 u (without internal calibration).

Total organic carbon (TOC) was measured using a Shimadzu TOC-5000 analyzer (Milan, Italy, catalytic oxidation on Pt at 680°C). The calibration was performed using standards of potassium phthalate.

Inorganic ions formed during target molecule degradation were identified by ion chromatography analysis using a Dionex chomatograph (Thermo Scientific, Milan, Italy) equipped with a Dionex 40 ED pump, a Dionex 40 ED conductimetric detector, a Dionex Ion Pac AS9-HC 4 x 250 mm column, and Ion Pac ASRS-ULTRA 4 mm conductivity suppressor, using 9 mM Na_2CO_3 as eluent at 1 mL/min.

2.4. Toxicity

The acute toxicity of bisphenol E and S and their degradation products was assessed using a Microtox Model 500 toxicity analyzer (Milan, Italy). The analyses were performed by evaluating the bioluminescence inhibition assay in the marine bacterium *Vibrio fischeri* by monitoring changes in the natural emission of luminescent bacteria. Freeze-dried bacteria, reconstitution solution, diluent (2% NaCl) and an adjustment solution (non-toxic 22% sodium chloride) were obtained from Azur (Milan, Italy). Samples were tested in a medium containing 2% sodium chloride, and luminescence was recorded after 5, 15 and 30 minutes of incubation at 15°C. No substantial differences were

found between the three contact times; the results related to 15 minutes of contact are reported below. The luminescence inhibition percentage was determined by comparison with a non-toxic control.

3. RESULTS AND DISCUSSION

3.1. Photoinduced degradation of bisphenol S and E

The photocatalytic degradation of BPS and BPE achieved the complete abatement of BPS in 1h, while BPE took longer (2h, see Figure 1), which concurs with the literature data obtained with other AOP methods[21,22].

Considering the mineralisation of the two molecules, the total organic carbon (TOC) disappearance was complete after 3h for BPE. For BPS, about 50% of TOC was mineralised within 1h of irradiation, but it took up to 7 hours to achieve almost complete mineralisation (>95%). Therefore, most of the organic carbon in this timeframe must be attributed to the formation of transformation products. For BPS, the release of sulphur as sulphate ions took place gradually over time and reached stoichiometric release after 5h of treatment. These results are consistent with the analyses in LC/HRMS (see below), which reveal, at that irradiation time, the absence of compounds containing a sulphur atom.

Figure 1 here

Acute toxicity for BPS, BPE and their transformation products was also assessed using the *Vibrio fischeri* assay. The EC_{50} values were 15.4 mg L^{-1} for BPS and 7.6 mg L^{-1} for BPE, thus implying that BPE is more toxic than BPS. For both compounds, the initial stages of the transformation involved the formation of TPs that were more toxic than the parent compound, as assessed by the higher percentage of inhibition and, after only 15 minutes of irradiation, the maximum value was achieved (100% of effect for BPE and 87% for BPS). Subsequently, the toxic effect decreased over time as the degradation products responsible for this increase in toxicity underwent mineralisation; in fact, the final points displayed negligible toxicity, which fits well with the achievement of complete mineralisation.

3.2. High-resolution Mass Spectrometry characterisation of bisphenol E and S

In order to identify and to establish the structural formulae of the TPs of BPS and BPE after the photocatalytic experiment, a thorough investigation of the MS^n fragmentation behaviour of the two molecules was performed. Analyses of BPE and BPS were carried out by HPLC/HRMS in ESI negative mode and their MS^n studies were instigated in CID mode with a collision energy of 15V aimed at establishing their characteristic fragments, very useful for identifying the structure of degradation products.

From low-energy CID MS/MS experiments, precursor deprotonated ions from BPS and BPE underwent several radical losses with the formation of abundant radical ions (illustrated in Table S1) and the proposed fragmentation pathways are shown in Figure 2. The ESI-MS of BPS indicated the formation of $[M-H]^-$ deprotonated molecule at *m/z* 249.0223. The product ion scan of the $[M-H]^-$ precursor ion produced four well-defined product ions: two radical product ions at *m/z* 108.0212[23] (base peak) and at *m/z* 184.0514 and two even electron product ions at *m/z* 155.9874 and 185.0591. The typical isotopic pattern of sulphur sustained by the accurate full mass data demonstrated that only the fragment at *m/z* 155.9874 still contains the sulphur atom within its structure.

Figure 2 here

The ESI-MS of BPE afforded the $[M-H]^-$ deprotonated molecule at *m/z* 213.0896. The product ion scan of the deprotonated molecule formed the main product ion at *m/z* 198.0665[23] which resulted by loss of a methyl radical (15.0231 Da), in addition to two low abundance product ions at *m/z* 119.0506 and 93.0356 which were formed by cleavage of the phenol portion and subsequent formation of phenolate ion.

3.3. Structural elucidation of transformation products for Bisphenol S

The process of identification of unknown transformation products was based on comparison of HPLC-ESI-HRMS chromatograms before and after photo-induced degradation. As described by Zhu *et al.* [24] the study of degradation processes by photocatalysis brought to a customized list of the main unknown *m/z* values of the hypothetic transformation products. We defined a customized list of possible TPs originated from bisphenol molecules based on known mass defect filtering. The customized list of suspected TPs was prepared using Xcalibur software (Xcalibur 4.1). By the use of the same software, additional non-target analytes were identified after manual inspection of the chromatograms. Three technical replicates for each time point were performed.

Twelve degradation products were detected during the treatment of bisphenol S, shown by the chromatographic profile reported in Figure S1, obtaining, on the basis of accurate mass value, their corresponding empirical formulae (see Table 1). The MS^2 and MS^3 spectra analysis of each identified TP deprotonated ion allowed us to assign a tentative structure for most of the transformation products; all MS^n ions are reported in Table S2 as Supplementary Information.

Two isomeric species at *m/z* **265.0164** (TP 266) with empirical formula $C_{12}H_9O_5S$ were detected and attributed to hydroxy-BPS. The radical hydroxylation process by photocatalysis is known not to be regiospecific, so any position on the aromatic rings could be a candidate for hydroxylation. Thanks to the symmetry of the molecule, the hydroxyl group could be properly located in the two isomers, and isomer A could be postulated as 3-hydroxy BPS and isomer B as 2-hydroxy BPS (see Scheme 1).

MS^2 spectrum of the precursor ion at 265 *m/z* closely resembled the fragmentation of BPS deprotonated molecule, but the introduction of a new OH group led to some differences (see Figure S2). The product ion at *m/z* 171.9831 (base peak) was due to the loss of phenol, namely the ring not subjected to hydroxylation. The product ion at *m/z* 108.0212 accounted for the unsubstituted ring while the product ion at *m/z* 124.0173 accounted for the hydroxylated ring. These three product ions are all associated by peaks at M-1 with lower intensity (at 171, 107 and 123 *m/z* respectively), due to the loss of $H^{\bullet}$ which leads to the formation of double bond by electron pairing of a double bond between carbon and oxygen in ortho or para position with respect to the sulphate group. Reaction (1) shows as an example of this mechanism occurring on the radical ion at *m/z* 171.9831 originating *m/z* 170.9714 and the corresponding resonance structures.

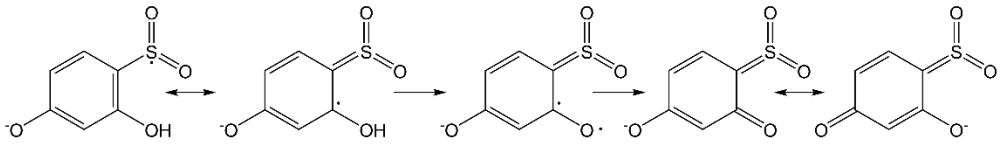

(1)

Five TPs involved ring opening reactions, namely TP 282 (*m/z* 281.0104), 216 (*m/z* 214.9999), 218 (*m/z* 217.0151), 254 (*m/z* 253.0155) and 284 (*m/z* 283.0215). All of the hypothesized structures are reported in Scheme 1. TP 282 originates a deprotonated ion at *m/z* 281.0104. The species with *m/z* **281.0104** and empirical formula $C_{12}H_9O_6S$ matched with the addition of two oxygen atoms to the parent molecule with the resulting ring opening. In this case, MS^2 spectrum was significantly changed respect to the one of BPS deprotonated ion, in line with a large modification of the parent molecule. In particular, the loss of formic acid accords with the formation of a carboxylic group subsequent to the ring opening. This loss is uncommon, especially respect to other hypothesized carboxylic structures, that show CO_2 loss. The other losses involved the detachment of SO_2 [25], which gave the fragment at *m/z* 217.0487, and the concerted loss of SO_2 and CO, coherent with the presence of a carbonyl group; these structural diagnostic ions allowed us to put forward the structure shown in Figure 3 (top).

Figure 3 here

A species with *m/z* **214.9999** and empirical formula $C_8H_7O_5S$ was formed from TP 216 and also enclosed a carboxylic group. The MS^2 spectrum of *m/z* 214.9999 gave the fragment at *m/z* 171.0111, through the neutral loss of carbon dioxide (43.9881 Da) originating from the detachment of the carboxylic group, and the fragment at *m/z* 93.0345 corresponding to phenolate ion, thus implying that one of the two phenolic rings had not been modified. Based on all these considerations, we proposed the structure displayed in Figure 3 (bottom).

The TP weighting 218 Da originated a deprotonated ion with *m/z* **217.0151** and empirical formula $C_8H_9O_5S$. It could be a typical gem-diol, i.e. a hydrate of the corresponding aldehyde. Respect to the parent compound, it displays a deeply changed fragmentation pathway, probably instigated by the negative charge located on the phenolic ring. MS^2 spectrum of molecular deprotonated ion exhibited three fragments at *m/z* 199.0045 deriving from a loss of water, at *m/z* 171.0111 through

the neutral loss of formic acid, and at *m/z* 93.0345 corresponding to the phenolate ion (see Figure S3). To explain these losses in the MS^2 spectrum, we highlight a dehydration reaction with the formation of a double bond to justify the loss of water, while keto-enolic tautomerism will produce the corresponding aldehyde; the loss of CO_2 could occur *via* a McLafferty rearrangement mechanism.

The two deprotonated ions at *m/z* **253.0155** and **283.0215** derive from TPs 254 and 284. These ions with empirical formulae $C_{11}H_9O_5S$ and $C_{12}H_{11}O_6S$ reveal in their MS^2 spectra fragments at *m/z* 155.9874, 108.0212 and 93.0345 (Figure S4-S5), all due to the presence of an unmodified phenolic ring. The absence of other diagnostic ions prevented us from identifying the portion of molecule subject to modification that carried out the detachment of one of the two phenolic rings. Therefore, the structures proposed in Scheme 1 are only partially defined.

A deprotonated ion with *m/z* **305.0311** (corresponding to TP 306) and empirical formula $C_{11}H_{13}O_8S$ reasonably underwent the opening of both aromatic rings. In fact, the absence of all peculiar ions perceived from BPS coupled with the decrease in DBE from 8 to 5 suggested a possible opening of both phenolic rings. As for the losses recorded in MS^2 of precursor ion at 305 *m/z* (see Figure S6), we identified the detachment of a water molecule to produce the fragment at *m/z* 287.0198, and the concerted loss of a water molecule and ketene; unfortunately, this information was not sufficient to define a structure uniquely.

The third family of compounds was made up of all those degradation products that undertook the detachment of one of the two phenolic rings, namely TP 174 (*m/z* 172.9900), 190-A and B (*m/z* 188.9851) and 222 (*m/z* 220.9748).

The deprotonated molecule at *m/z* **172.9900** (related to TP 174) with empirical formula $C_6H_5O_4S$ is formed through the detachment of one of the two aromatic rings and was attributed to 4-phenolsulphonic acid. In close analogy with the MS spectrum originated from BPS ionization, it also presented a signal at *m/z* 346.9873 corresponding to its dimeric form.

Two isomeric BPS derivatives, named TP 190-A and TP 190-B are recognized from their deprotonated species at *m/z* **188.9851** with empirical formula $C_6H_5O_5S$. They derive from the hydroxylation of TP 174. Based on the retention times, we attributed 190-A to 2,4-dihydroxybenzenesulfonic acid. TP 190-B revealed a retention time longer than TP 174, which may be justified by the proximity of the two OH groups on the aromatic ring, which decreases the TP

polarity by forming an intramolecular hydrogen bond. We therefore hypothesised the 3,4-dihydroxybenzenesulfonic acid structure for TP 190-B.

The final intermediate belonging to this group is TP 222, whose deprotonated ion at *m/z* **220.9748** correspond to an empirical formula $C_6H_5O_7S$. By CID MS^2 of *m/z* 220.9748 ion, we noted the appearance of a fragment at *m/z* 122.9752, formed through the loss of $C_4H_2O_3$ (97.9962 Da). This is well-matched with the ring opening and was attributed to two tentative structures, as shown in Figure 4.

Figure 4 here

The sum of the tentative transformation pathways followed by BPS is illustrated in scheme 1 and takes account of the formation and disappearance kinetics of the intermediates characterised thus far. The kinetics of evolution of the concentration of the intermediates was followed by HPLC-ESI HRMS, by recording in function of time the data corresponding to the chromatographic peak areas of each deprotonated molecule. The evolution profiles of the TPs are shown in Figure S7 and the majority display a maximum of around 25-30 minutes and complete disappearance within 2h of irradiation. TP 174 was the most abundant by-product, while all other TPs exhibited similar relative abundance, thus implying that the cleavage of the molecule at the level of the sulphur atom is a very important transformation route; later, it underwent progressive oxidation.

Scheme 1 here

The other key reactions were the hydroxylation of the substrate to give mono- and poly-hydroxylated BPs and the ring cleavage, as most of the detected TPs derived from these reactions.

3.4. Structural elucidation of the transformation products and transformation pathways for Bisphenol E

Ten transformation products were detected following BPE degradation *via* HPLC-HRMS analysis (see Figure S8). The accurate mass for each TP-derived ion was established, allowing us to obtain the empirical formulae for all by-products, as illustrated in Table 2. MS^2 and MS^3 spectra analysis were

performed to all of the identified deprotonated molecular ions and the procedure allowed for a tentative structure to be assigned for most of the transformation products and all MS^n ions are reported in Table S3 as Supplementary Information.

We detected three species, identified as TP 230, TP246 and TP 262 at *m/z* **229.0839**, **245.0789** and **261.0725.** The *m/z* ratio values matched with the elemental composition $C_{14}H_{13}O_3$, $C_{14}H_{13}O_4$ and $C_{14}H_{13}O_5$ consistent with the monohydroxy, dihydroxy and trihydroxy-BPE, respectively. A *ortho*-monohydroxylated derivative was also detected among the biotransformation products of BPE through the biphenyl-degrading bacterial strain[26]. With regard to the TP 230 originating a deprotonated molecule at *m/z* **229.0839**, we can exclude a hydroxylation on the methyl group thanks to the presence of the methyl loss in MS^2 spectrum of precursor ion *m/z* 229.0839 itself (see Figure S9). The other losses involved the detachment of the ring with or without the OH group, but did not provide useful information for the structural examination.

In the cases of identified TPs 246 and 262, the absence of product ion signals in their MS^2 induced fragmentation prevented us from obtaining information on the localisation of the OH groups.

We identified seven TPs at lower molecular weight, whose formation accounts for the molecule breakage. Two isomeric species were defined as TP 220-A and TP 220-B with *m/z* **219.0639** and formula $C_{12}H_{11}O_4$. They involved the cleavage of one of the aromatic rings and both their MS^2 spectra revealed a product ion at *m/z* 175.0749 formed through the loss of CO_2, consistent with a terminal carboxylate group (see Figure S10).

Two isomeric species were identified as TP 236-A and TP 236-B. The relative precursor ions at *m/z* **235.0579** with formula $C_{12}H_{11}O_5$ matched with the hydroxylation of one of the TPs 220, but the absence of MS^2 detectable product ions prevented us from properly locating the hydroxyl groups.

TP 244 originated a deprotonated molecule at *m/z* **243.0625** with empirical formula $C_{14}H_{11}O_4$. The fragmentation of *m/z* 243 precursor ion exhibited several structural-diagnostic product ions in its MS^2 spectrum (see Figure S11). The product ion at *m/z* 149.0236 was well-harmonised with the presence of an unmodified phenolic ring, while the loss of methyl radical (product ion at *m/z* 228.0396) was coherent with the presence of unmodified methyl in the bridge. The other losses came from the portion of the molecule subjected to the ring opening and suggested:

1) the presence of a carboxylic group, as demonstrated by the loss of CO_2, with the formation of the product ion at *m/z* 199.0742;

2) the presence of a terminal carbonyl group thanks to the losses of CO and a molecule of water (product ions at *m/z* 215.0685 and 225.0526).

We tentatively hypothesised the structure reported in Figure 5.

Figure 5 here

TP 260, corresponding to a deprotonated molecule at *m/z* **259.0569** and formula $C_{14}H_{11}O_5$, arose from TP 244 following hydroxylation, but the absence of any MS^n signal prevented the structural elucidation.

All these TPs are illustrated in Scheme 2. BPE transformation proceeded mainly through an oxidative pathway.

Scheme 2 here

The evolution of the TPs over time followed typical bell-shaped profiles, with the maximum amount reached in 15 minutes for TP 230 and 220, while the other TPs were formed at a slower rate, this implying that they arose from a modification of these TPs through further hydroxylation. Hence, we can state that TPs 236 and 260 arose from 220 and 236, respectively (maximum achieved after 30 minutes).

The two main routes were the hydroxylation and ring opening, with the formation of TPs 220 and 244, further transformed into TPs 236 and 260.

CONCLUSIONS

The HPLC/HRMS method we developed was useful for characterising and identifying newly-formed TPs from bisphenol S and E exploiting the high resolving power of the orbitrap to hypothesise their structural formulae. In fact, this study allowed us to investigate around twenty transformation products detected during TiO_2 mediated photolysis treatment and, by coupling this with the

evolution profile, we were able to propose possible transformation routes. In the case of BPS, the two most likely preferred degradation pathways were mono-hydroxylation and cleavage at the level of the sulphur atom with loss of one of the two rings and formation of a sulphate group, as already reported for different oxidation and sonolytic processes[27], while, for BPE, the two main processes involved hydroxylation and ring-opening. Although an increase in acute toxicity was observed during the early phase of treatment, the mineralisation of the compounds was achieved after a lengthy irradiation time.

Future developments will need to focus on ascertaining which of the identified by-products contribute most to the toxicity highlighted during the treatment and on attempting to assess if there is correspondence between the intermediates observed in this simpler system and those that can be formed in more complex real aqueous matrices (e.g. wastewater).

REFERENCES

1. Abts G, Eckel T, Wehrmann R. Polycarbonates. In: *Ullmann's Encyclopedia of Industrial Chemistry*. American Cancer Society; 2014:1-18. doi:10.1002/14356007.a21_207.pub2

2. Almeida S, Raposo A, Almeida-González M, Carrascosa C. Bisphenol A: Food Exposure and Impact on Human Health. *Compr Rev Food Sci Food Saf*. 2018;17(6):1503-1517. doi:10.1111/1541-4337.12388

3. Corrales J, Kristofco LA, Steele WB, et al. Global Assessment of Bisphenol A in the Environment: Review and Analysis of Its Occurrence and Bioaccumulation. *Dose-Response*. 2015;13(3):1559325815598308. doi:10.1177/1559325815598308

4. Magi E, Scapolla C, Di Carro M, Liscio C. Determination of endocrine-disrupting compounds in drinking waters by fast liquid chromatography–tandem mass spectrometry. *J Mass Spectrom*. 2010;45(9):1003-1011. doi:10.1002/jms.1781

5. Staples CA, Dorn PB, Klecka GM, O'Block ST, Harris LR. A review of the environmental fate, effects, and exposures of bisphenol A. *Chemosphere*. 1998;36(10):2149-2173. doi:10.1016/S0045-6535(97)10133-3

6. Rezg R, El-Fazaa S, Gharbi N, Mornagui B. Bisphenol A and human chronic diseases: Current evidences, possible mechanisms, and future perspectives. *Environ Int*. 2014;64:83-90.

doi:https://doi.org/10.1016/j.envint.2013.12.007

7. Skakkebæk NE, Rajpert-De Meyts E, Main KM. Testicular dysgenesis syndrome: an increasingly common developmental disorder with environmental aspects: Opinion. *Hum Reprod*. 2001;16(5):972-978. doi:10.1093/humrep/16.5.972

8. Matuszczak E, Komarowska MD, Debek W, Hermanowicz A. The Impact of Bisphenol A on Fertility, Reproductive System, and Development: A Review of the Literature. *Int J Endocrinol*. 2019;2019:4068717. doi:10.1155/2019/4068717

9. Commission Directive 2011/8/EU amending Directive 2002/72/EC as regards the restriction of use of Bisphenol A in plastic infant feeding. *Off J Eur Union L 26*.:11-14.

10. Onghena M, Van Hoeck E, Van Loco J, et al. Identification of substances migrating from plastic baby bottles using a combination of low-resolution and high-resolution mass spectrometric analysers coupled to gas and liquid chromatography. *J Mass Spectrom*. 2015;50(11):1234-1244. doi:10.1002/jms.3644

11. Chen D, Kannan K, Tan H, et al. Bisphenol Analogues Other Than BPA: Environmental Occurrence, Human Exposure, and Toxicity—A Review. *Environ Sci Technol*. 2016;50(11):5438-5453. doi:10.1021/acs.est.5b05387

12. Choi YJ, Lee LS. Partitioning Behavior of Bisphenol Alternatives BPS and BPAF Compared to BPA. *Environ Sci Technol*. 2017;51(7):3725-3732. doi:10.1021/acs.est.6b05902

13. Wang H, Liu Z, Tang Z, et al. Bisphenol analogues in Chinese bottled water: Quantification and potential risk analysis. *Sci Total Environ*. 2020;713:136583. doi:https://doi.org/10.1016/j.scitotenv.2020.136583

14. Noszczyńska M, Piotrowska-Seget Z. Bisphenols: Application, occurrence, safety, and biodegradation mediated by bacterial communities in wastewater treatment plants and rivers. *Chemosphere*. 2018;201:214-223. doi:https://doi.org/10.1016/j.chemosphere.2018.02.179

15. Wang H, Liu Z, Zhang J, et al. Insights into removal mechanisms of bisphenol A and its analogues in municipal wastewater treatment plants. *Sci Total Environ*. 2019;692:107-116. doi:https://doi.org/10.1016/j.scitotenv.2019.07.134

16. Sun Q, Wang Y, Li Y, et al. Fate and mass balance of bisphenol analogues in wastewater treatment plants in Xiamen City, China. *Environ Pollut*. 2017;225:542-549. doi:https://doi.org/10.1016/j.envpol.2017.03.018

17. Rosenmai AK, Dybdahl M, Pedersen M, et al. Are Structural Analogues to Bisphenol A Safe Alternatives? *Toxicol Sci*. 2014;139(1):35-47. doi:10.1093/toxsci/kfu030

18. Pelch KE, Li Y, Perera L, Thayer KA, Korach KS. Characterization of Estrogenic and Androgenic Activities for Bisphenol A-like Chemicals (BPs): In Vitro Estrogen and Androgen Receptors Transcriptional Activation, Gene Regulation, and Binding Profiles. *Toxicol Sci*. 2019;172(1):23-37. doi:10.1093/toxsci/kfz173

19. Calza P, Vione D, Galli F, Fabbri D, Dal Bello F, Medana C. Study of the photochemical transformation of 2-ethylhexyl 4-(dimethylamino)benzoate (OD-PABA) under conditions relevant to surface waters. *Water Res*. 2016;88. doi:10.1016/j.watres.2015.10.015

20. Avetta P, Bianco Prevot A, Fabbri D, Montoneri E, Tomasso L. Photodegradation of naphthalene sulfonic compounds in the presence of a bio-waste derived sensitizer. *Chem Eng J*. 2012;197:193-198. doi:10.1016/j.cej.2012.04.086

21. Wang G, Wu F, Zhang X, Luo M, Deng N. Enhanced TiO_2 photocatalytic degradation of bisphenol E by β-cyclodextrin in suspended solutions. *J Hazard Mater*. 2006;133(1):85-91. doi:https://doi.org/10.1016/j.jhazmat.2005.09.058

22. Zhang D, Lee C, Javed H, Yu P, Kim J-H, Alvarez PJJ. Easily Recoverable, Micrometer-Sized TiO2 Hierarchical Spheres Decorated with Cyclodextrin for Enhanced Photocatalytic Degradation of Organic Micropollutants. *Environ Sci Technol*. 2018;52(21):12402-12411. doi:10.1021/acs.est.8b04301

23. Cao X-L, Kosarac I, Popovic S, Zhou S, Smith D, Dabeka R. LC-MS/MS analysis of bisphenol S and five other bisphenols in total diet food samples. *Food Addit Contam Part A*. 2019;36(11):1740-1747. doi:10.1080/19440049.2019.1643042

24. Zhu M, Ma L, Zhang D, Ray K, Zhao W, Humphreys G, Skiles G, Sanders M, Zhanh H. Detection and Characterization of Metabolites in Biological Matrices Using Mass Defect Filtering of Liquid Chromatography/High Resolution Mass Spectrometry Data. *Drug Metab Dispos*. 2006;34(10):1722-1733. doi:10. 1124/dmd.106.009241.

25. Giancotti V, Medana C, Aigotti R, Pazzi M, Baiocchi C. LC-high-resolution multiple stage spectrometric analysis of diuretic compounds. Unusual mass fragmentation pathways. *J Pharm Biomed Anal*. 2008;48(2):462-466. doi:10.1016/j.jpba.2008.03.014

26. Zühlke M-K, Schlüter R, Mikolasch A, et al. Biotransformation of bisphenol A analogues by the biphenyl-degrading bacterium Cupriavidusbasilensis - a structure-biotransformation relationship. *Appl Microbiol Biotechnol*. 2020;104(8):3569-3583. doi:10.1007/s00253-020-10406-4

27. Lu X, Zhao J, Wang Q, et al. Sonolytic degradation of bisphenol S: Effect of dissolved oxygen and peroxydisulfate, oxidation products and acute toxicity. *Water Res*. 2019;165:114969. doi:https://doi.org/10.1016/j.watres.2019.114969

Tables

$[M-H]^-$	Empirical formula	Δppm	RT (min)
172.9900	$C_6H_5O_4S$	-1.8	1.83
188.9851 (A, B)	$C_6H_5O_5S$	-0.6	1.83; 2.35
214.9999	$C_8H_7O_5S$	-4.5	2.86
217.0151	$C_8H_9O_5S$	-6.6	4.92
220.9748	$C_6H_5O_7S$	-1.1	1.66
253.0155	$C_{11}H_9O_5S$	-4.0	7.81
265.0164 (A, B)	$C_{12}H_9O_5S$	-0.5	10.61; 11.05
281.0104	$C_{12}H_9O_6S$	-3.7	9.06
283.0215	$C_{12}H_{11}O_6S$	-19.7	6.79
305.0311	$C_{11}H_{13}O_8S$	-4.8	3.56

Table 1: BPS and its transformation products formed during the photocatalytic process.

$[M-H^-]$	Empirical formula	Δppm	t_r (min)
219.0639 A, B	$C_{12}H_{11}O_4$	-5.9	12.01; 12.22
229.0839	$C_{14}H_{13}O_3$	-8.8	15.08
235.0579 A, B	$C_{12}H_{11}O_5$	-9.4	10.69; 12.05
243.0625	$C_{14}H_{11}O_4$	-11.0	14.97
245.0789	$C_{14}H_{13}O_4$	-7.9	9.93
259.0569 A, B	$C_{14}H_{11}O_5$	-12.3	14.70; 16.40
261.0725	$C_{14}H_{13}O_5$	-12.4	12.39

Table 2*:* Transformation products formed from BPE

Figure captions

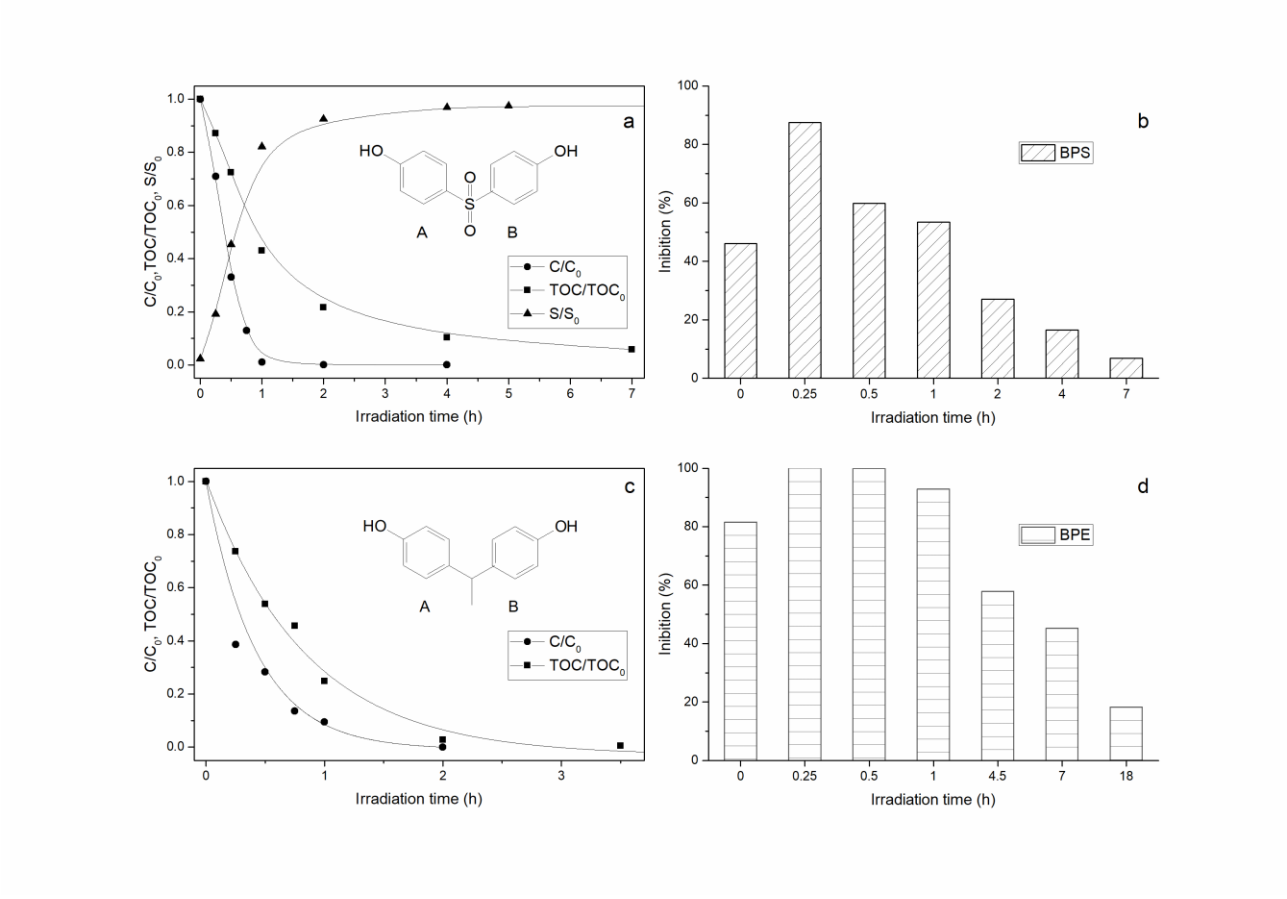

Figure 1: Bisphenol S (top, a and b) and Bisphenol E (bottom, c and d) disappearance (C/C_0, ●), mineralization (TOC/TOC_0, ■), sulphate evolution (S/S_0, ▲) and toxicity (% inhibition) as a function of the irradiation time in the presence of TiO_2.

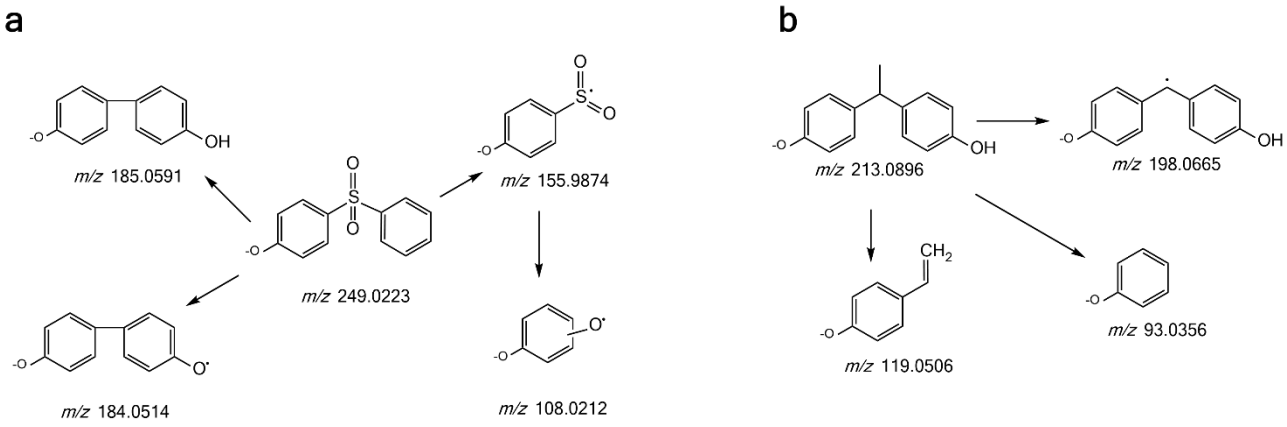

Figure 2: CID-MS/MS fragmentation pathways for bisphenol S (a) and E (b).

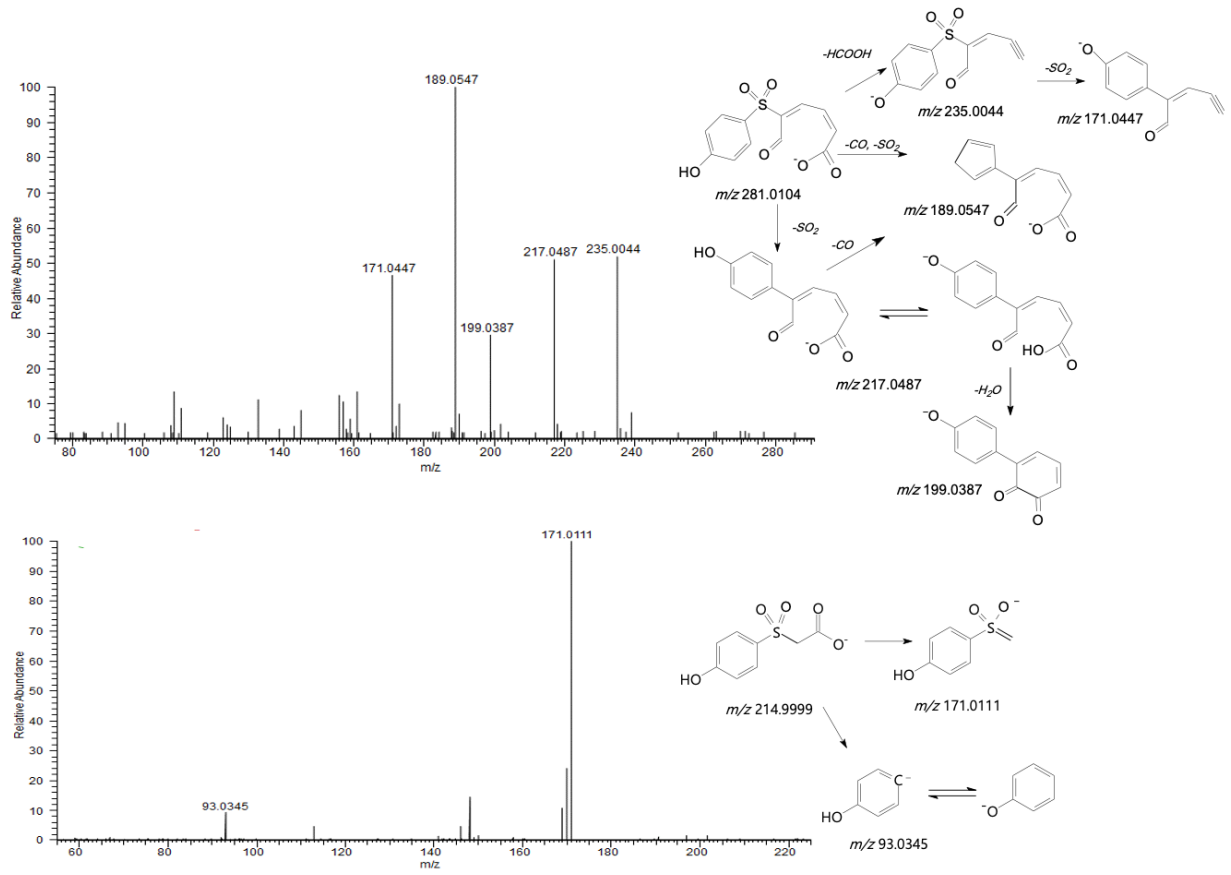

Figure 3. CID-MS/MS spectrum and proposed fragmentation pathways for TP 282 (m/z 281.0104) (top) and TP 216 (m/z 214.9999) (bottom).

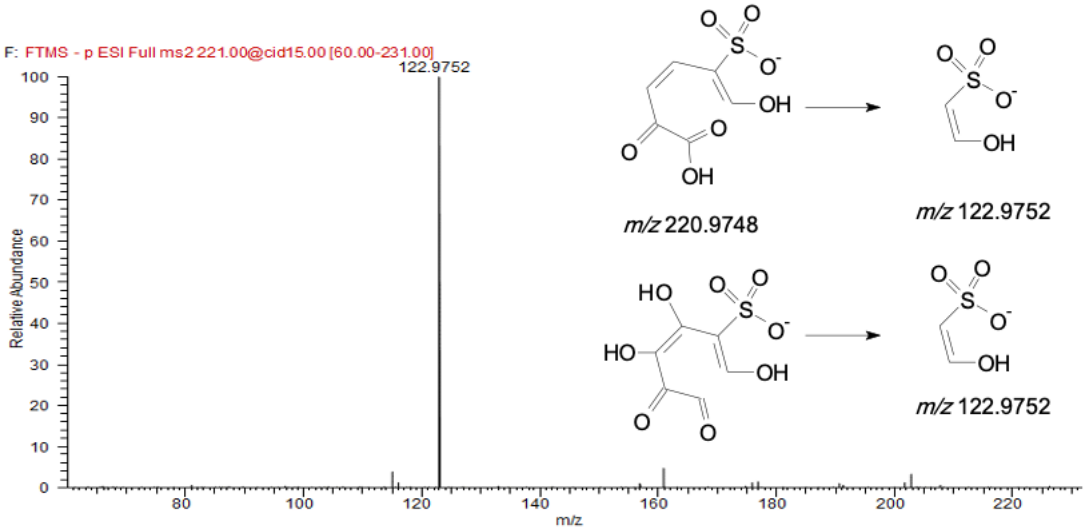

Figure 4. CID-MS/MS fragmentation spectrum and proposed fragmentation pathways for transformation product with *m/z* 220.9748 (TP 222).

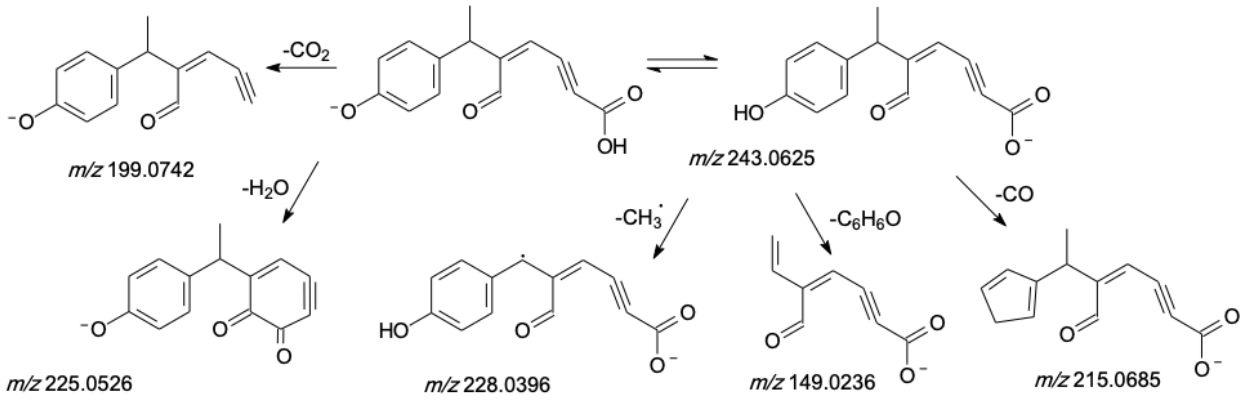

Figure 5: Proposed fragmentation pathways for TP 244 with *m/z* 243.0625.

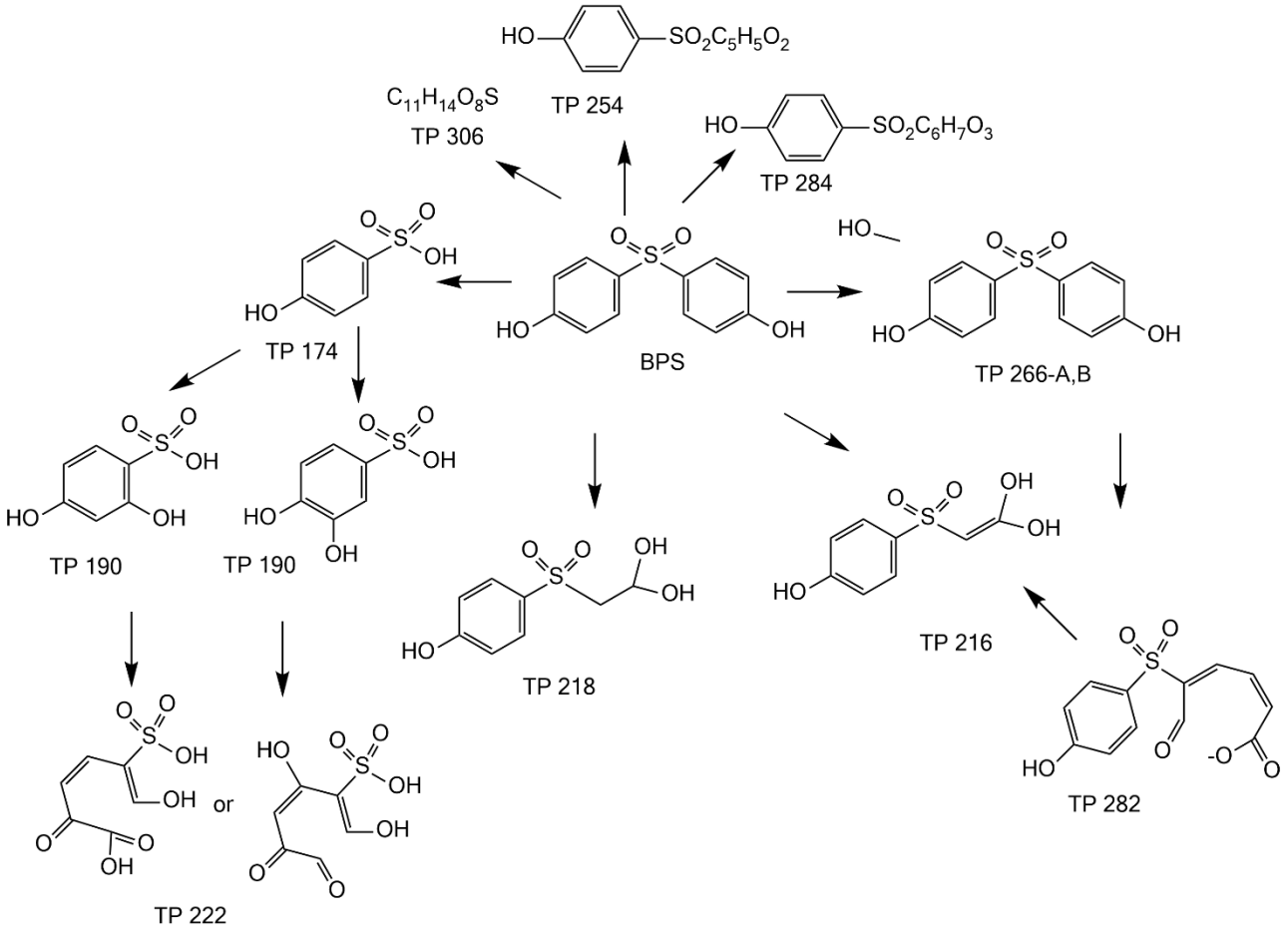

Scheme 1: Proposed photoinduced degradation pathways for BPS.

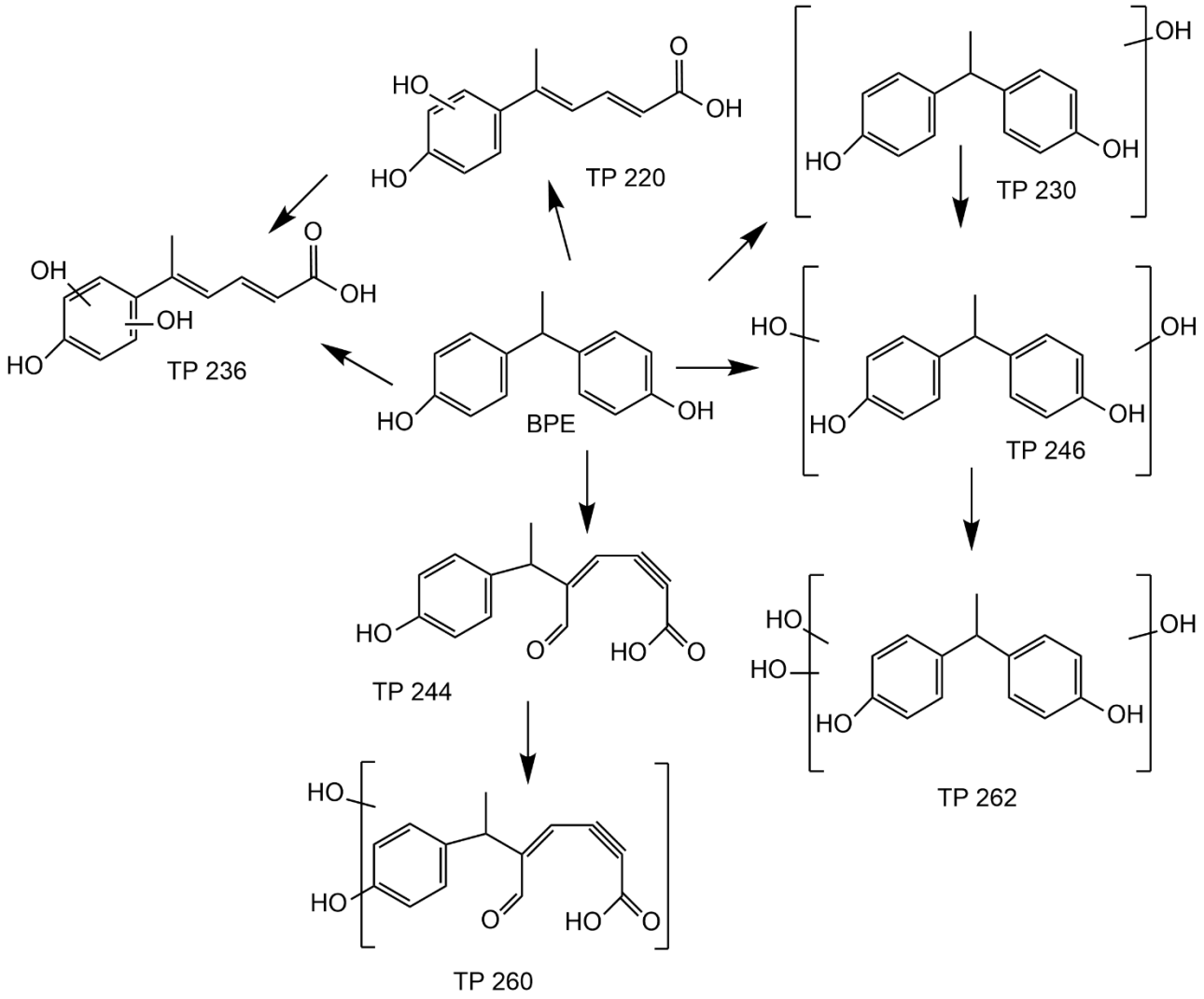

Scheme 2: Proposed photoinduced degradation pathways for BPE